JOURNAL OF Applied Polymer SCIENCE

Toughening mechanism of PPS/Sr ferrite composites by TPU elastomer

Liang Qiao, Xin Dong, Yao Ying, Jingwu Zheng, Wangchang Li, Shenglei Che
College of Materials Science and Engineering, Zhejiang University of Technology, Hangzhou 310014, China
Correspondence to: S. Che (E-mail: cheshenglei@zjut.edu.cn)

ABSTRACT: In order to improve the impact strength of PPS-based strontium ferrite composite, the thermoplastic polyurethane (TPU) elastomer was added in the composite as a toughening agent. The composites were obtained by melt-blending PPS, TPU and strontium ferrites in twin-screw extruder. The crystalline state, thermal property, surface morphology and impact strength of the composites were investigated by using X-ray diffraction, differential scanning calorimetry, thermoravimetric analysis, scanning electron microscope and izod impact test. The addition of TPU improves impact strength of PPS-based strontium ferrite composite. When the addition of TPU increases to 11wt %, the impact strength of Sr-ferrite/PPS/TPU composite is enhanced by 51.44% compared with the sample without TPU addition, and reaches to 5.77 kJ/m^2. The occurrence of bonding interaction between PPS and TPU, demonstrated by a series of experiments, changes the structure and impact properties of PPS. Based on the experimental results, a possible mechanism is proposed to explain the improvement of Sr-ferrite/PPS/TPU composites, which is different from the conventional toughening mechanism by the conformation of elastomers and the suppression of microcracks propagation. © 2016 Wiley Periodicals, Inc. J. Appl. Polym. Sci. **2016**, *133*, 43564.

KEYWORDS: blends; crystallization; mechanical properties; morphology; thermal properties

Received 18 November 2015; accepted 16 February 2016
DOI: 10.1002/app.43564

INTRODUCTION

It has been more than half a century since bonded magnets were first developed by Baermann in 1934 in Germany. Polymer-bonded magnets have many variations and wide range of application. Bonded magnets acted as key components in electromechanical application. A lot of efforts have been done to manufacture "easy-to-use" magnets with high performance e.g., high dimensional preciseness, complicated shapes, thin-walled shapes, radially oriented anisotropic magnets for multipole magnetizing with inexpensive prices.[1,2] The mechanical properties such as high thermal stability, excellent electrical insulation, good chemical and flame resistance, and anti-aging of Polyphenylene sulfide (PPS) were excellent due to its rigid structure of thioether bond. It is widely used as special engineering plastic in the field of aerospace, electronic information engineering, auto mechanics, textile and clothing. The global demand for PPS was estimated to maintain an annual growth rate of 10%.[3–5] With the demand increases of plastic magnets in the field of high temperature, more and more researchers focused their attentions on the development of plastic magnets made by PPS.

However, the large brittleness and weak toughness of PPS confine its high-end applications. To overcome these deficiencies, modification of PPS with elastomers,[6] inorganic particles,[7] glass fiber[8] or carbon fiber[9] by melt blending developed rapidly in recent years and showed remarkable reinforcing effects on the mechanical, thermal, and wear properties. These toughening methods are based on different conventional toughening mechanism, such as elastomers toughening theory,[10] cold drawing concept, crazing theory and shear band/crazing interaction theory.[11] However, the toughening methods via glass fibers or carbon fibers are hard to be applied on account of the limitation of the filler contents in the field of high filling functional composites. Thermoplastic polyurethane (TPU), which possesses excellent combined performances in toughness, durability, flexibility, biocompatibility, and biostability, is applied to toughen polypropylene (PP), poly vinylidene fluoride (PVDF), polyamide (PA), polyacetal and so on.[12–14] However, the application of TPU in toughening PPS is seldom reported possibly considering the relative poor high temperature stability. In this paper, the strong toughening effect was found in Sr-ferrite/PPS/TPU composite system and the influence mechanism of TPU on PPS-based composites was also explored.

EXPERIMENTAL

Preparation of Sr-Ferrite/PPS/TPU Composites and PPS/TPU Composites

1290 g commercial Sr-ferrites modified by KH550 coupling agent (Zhejiang Li Chuang Inc.), 210 g polymers containing PPS (V-100, TOSOH) with the molecular weight of 4000∼5000 and the density of 1.34 g/cm^3 and TPU (3092, Shanghai Hiend

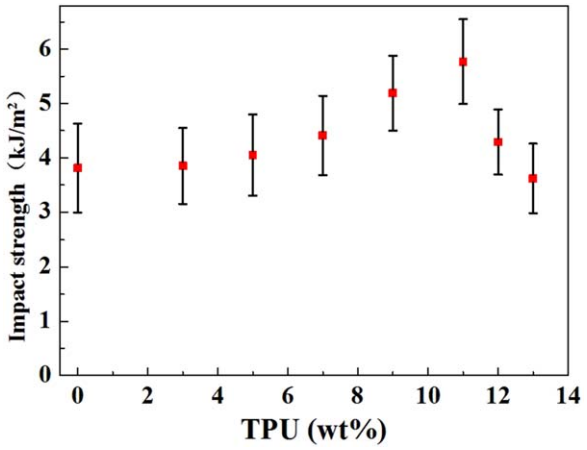

Figure 1. The IS of Sr-ferrite/PPS/TPU composites with different TPU contents (the error bars are standard deviations). [Color figure can be viewed in the online issue, which is available at wileyonlinelibrary.com.]

polyurethane Inc. polyether) with the density of 1.18 g/cm^3 were stirred well in the mixer. The TPU contents varied from 1 to 12 wt % of the PPS content. After dried at 100 °C for 4 hours, the mixtures were blended to get the pea-sized pellets in the twin-screw extruder at the different temperatures between 265 and 300 °C, which were then injected into different samples for the measurements. To investigate the properties of the TPU-modified PPS matrix, PPS/TPU composites with different TPU contents from 10 to 30 wt % were melt-blended at 290 °C by using HAAKE torque rheometer.

Characterization

Thermogravimetric analysis was measured on the IR/TG thermobalance equipment (Q5000) under atmosphere with the heating rate of 10 °C/min. The crystallinity and melting behavior of PPS/TPU composites were investigated by using differential scanning calorimetry (DSC) (Mettler STA7300) under flowing nitrogen. The crystallinity ΔX of PPS in composites was calculated with the following formula:

$$X_d = \Delta H_m / \Delta H* \quad (1)$$

Where ΔH_m is the melting enthalpy of PPS in the composites, and ΔH^* is the melting enthalpy of perfect crystallization of pure PPS ($\Delta H^* = 94.96$ J/G).[15]

Rectangular specimens (80 × 10 × 4 mm^3) of Sr-ferrite/PPS/TPU samples were prepared for the non-notched impact strength (IS) measurement in accordance with GB/T 1043.1-2008 by radial-boom impact tester (SNAS JBW300). The number of samples tested in the impact tests were twelve. The transverse impact energy was given at 25 °C during testing and the mean values of IS were calculated after deleting the maximum and minimum values. The samples were tested in random order to avoid the blocking effects. Fourier transform infrared spectrum (FTIR) was recorded on Bruker Vector 33 with KBr pellets and the wavelength ranging from 4000 cm^{-1} to 400 cm^{-1}. The X-ray diffraction (XRD) analysis was performed by using X'Pert PRO, PANalytical (NED) to achieve the phase change. The fractural surfaces of impact testing specimens were treated by the gold sputtering for 60 s. Then the morphology was examined with a scanning electron microscope (Quanta 600).

RESULTS AND DISCUSSION

Figure 1 shows the effect of the TPU content on the IS of Sr-ferrite/PPS composites. Clearly, the addition of TPU enhances the IS gradually to a peak with TPU content of 11 wt %. The maximum IS of the composite with 11wt % TPU is improved by around 51.44% compared with the one without TPU addition. However, as the TPU content further increases to over 11 wt %, a sharp drop occurs in the IS. Therefore, moderate TPU addition improves the IS of the Sr-ferrite/PPS composites.

The fractural surfaces of the impact samples were shown in Figure 2. Morphology of these two specimens is similar and the Sr-ferrite particles are both coated with the PPS matrix. The sample modified with 11 wt % TPU is slightly rougher than that of the PPS/Sr-ferrite sample. There was no distinct proof to explain the toughness increase of the Sr-ferrite/PPS/TPU composites based on the SEM images. So it is necessary to discuss the system of PPS/TPU alone. In order to explore the toughening mechanism of PPS/Sr ferrite composites by TPU elastomer, we magnify the content of TPU from 10 to 30 wt %.

It is known that TPU is a block copolymer consisting of aromatic or aliphatic polyurethane as hard segments and aliphatic polyester or polyether as soft segments shown in Figure 3.[16] Derivative thermogravimetry (DTG) curve of TPU by a derivative formula is shown in Figure 4. It can be seen that the decomposition of TPU displays three stages occurring in the temperature range of

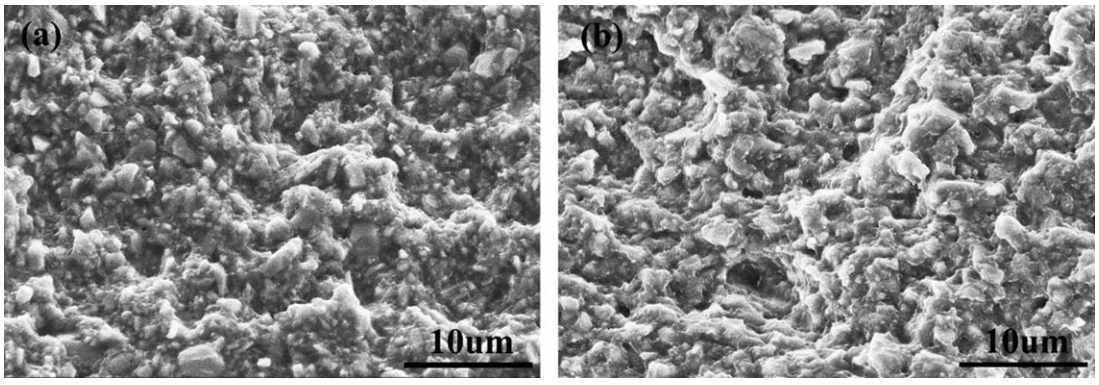

Figure 2. SEM micrographs of fractural surfaces of Sr-ferrite/PPS/TPU composites; (a) no TPU addition. (b) 11 wt % TPU addition.

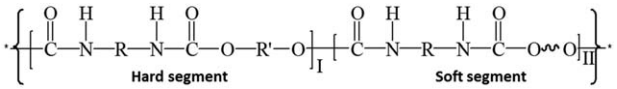

Figure 3. The structure of hard segment and soft segment of polyurethane.

261–356 °C, 356–427 °C and 427–500 °C, respectively. The DTG curve increases suddenly at 261 and 356 °C, which is associated with the decompositions of the hard and soft segments of TPU, respectively.[17] The sharp change above 427 °C in the DTG curve comes from the combustion of the decomposed fragments, which agrees with the results in the previous results.

Figure 5 shows the TGA and DTG curves of the PPS/TPU composites with different TPU contents. It can be seen from curve 1 that PPS starts to lose weight at about 435 °C, which displays the good high temperature property. The slight weight loss at 150 °C may be associated with the some matter with low volatility temperature in the raw material. In contrast, the single TPU sample starts to lose weight at a lower temperature of about 261 °C as shown in curve 5. When TPU is added in PPS, it does not influence the initial TGA change of composites, which still occurs at about 300 °C as shown in Figure 5 (curve 2, 3 and 4). However, with the temperature increasing, the TGA curves start to change differently, which implies that TPU has different decomposition behavior when it is added in PPS. It can be seen from curve 2, 3 and 4 that the decomposition of the PPS/TPU composites exhibits two stages apparently. The first stage is associated with the decomposition of hard segments and soft segments, which is similar with pure TPU. Nevertheless, the decomposition temperature is improved by almost 40 °C, which is ascribed to the protection of PPS covering TPU and possible chemical reaction between PPS and TPU. The second stage starts at the same temperature of around 435 °C as pure PPS, indicating that it is caused by the decomposition of PPS. However, it is noted that pure PPS has faster decomposition rate and more decomposition products than the PPS/TPU composites above 450 °C. This implies that TPU improves the stabilization of PPS during the final stage of the PPS degradation process.

Apart from the thermal stability, the crystallization behavior of the polymer matrix in the composites is also important when

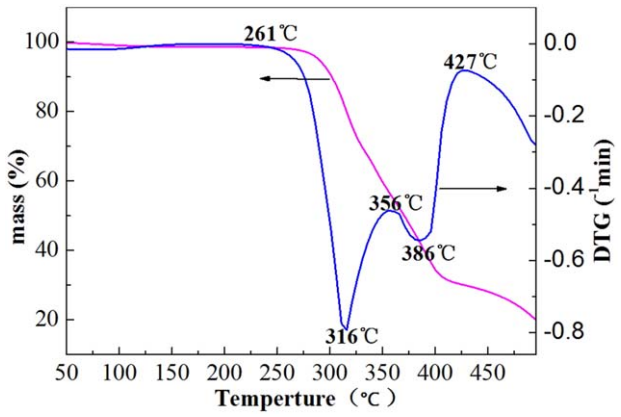

Figure 4. TGA and DTG curves of pure TPU in atmosphere. [Color figure can be viewed in the online issue, which is available at wileyonlinelibrary.com.]

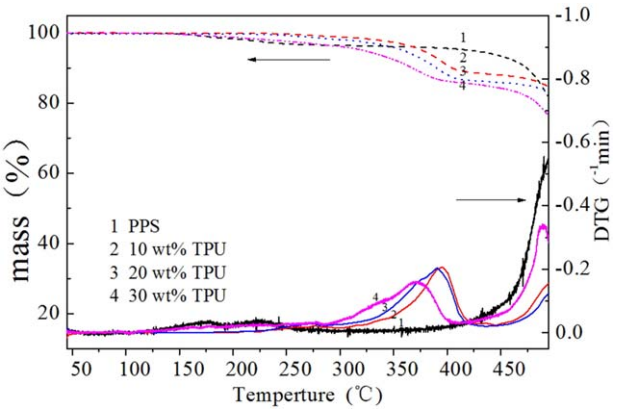

Figure 5. TGA and DTG curves of the TPU/PPS composites in oxygen atmosphere. [Color figure can be viewed in the online issue, which is available at wileyonlinelibrary.com.]

TPU exists. The crystallinity of PPS was discovered to be conspicuously raised by the presence of microscale or nanoscale fillers generally.[18,19] Figure 6 shows the DSC scans of PPS/TPU composites. A sharp endothermal peak appears in the curve of PPS at 282 °C, corresponding to the melting temperature (T_m). Oppositely, TPU shows no peak in the curve, which implies that TPU is amorphous. In the PPS/TPU composites system, only single prominent melting peak is observed, which indicates that there is no other crystallization phase forming in the PPS/TPU composite system. Furthermore, the melting temperatures shift to the lower temperature of about 278 °C regardless of the variation of the TPU concentration. This reveals that the system presents a new melting behavior different from the single PPS. In general, the high melting point is associated with the perfect crystallinity of PPS.[20] The calculated crystallinity of PPS with the addition of TPU decreases around 12.5%, and it keeps almost constant as the TPU concentration increases from 10 to 30 wt %. The addition of TPU into PPS may disrupt the folding of the PPS chains into crystals and limit their movements like carbon fibers[21] and consequently result in the decrease of the melting temperature and crystallinity of PPS.

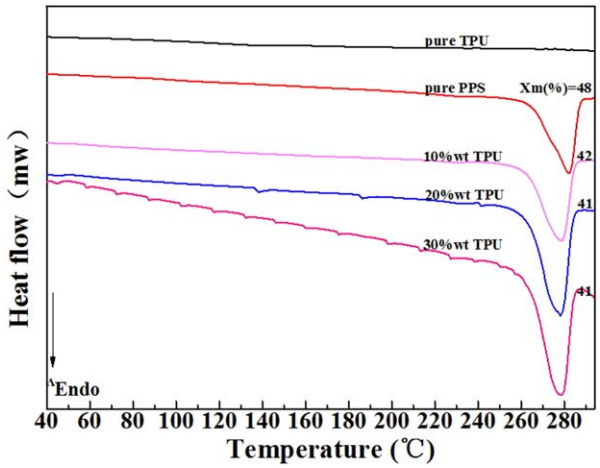

Figure 6. DSC curves of TPU, PPS and PPS/TPU composites. [Color figure can be viewed in the online issue, which is available at wileyonlinelibrary.com.]

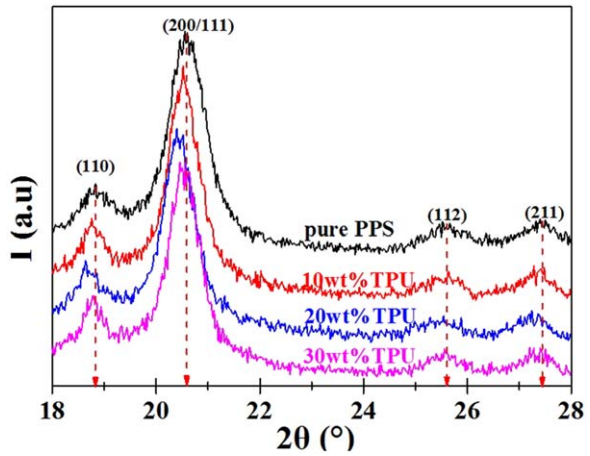

Figure 7. XRD patterns of PPS and PPS/TPU composites. [Color figure can be viewed in the online issue, which is available at wileyonlinelibrary.com.]

Another possibility that the crystal structure of PPS is changed by the addition of TPU must be considered. Figure 7 shows the XRD results of PPS/TPU composites. The four diffraction peaks at 18.83, 20.58, 25.62, and 27.42° corresponds to the (110), (200/111), (112) and (211) planes of the orthorhombic structure of PPS, respectively.[15] The PPS/TPU composites show the same diffraction peaks as the pure PPS. This illustrates that the PPS/TPU composites still possess the same crystal structure as PPS and no new phase forms. In the meantime, PPS/TPU diffraction peaks shift to the lower degree relative to PPS's corresponding peaks, which shows the slight change of PPS crystallization, which is in accordance with the results of differential thermal analysis.

Figure 8 shows the FTIR spectra of pure PPS, TPU and PPS/TPU samples Some characteristic peaks of pure PPS can be observed including C—C stretching vibrations peak [$\nu_{(C-C)}$] of benzene ring located at 1573, 1470 and 1387 cm^{-1}, C—S stretching vibration peak [$\nu_{(C-S)}$] at 1091 cm^{-1} C—H out-of-plane deformation vibration [$\gamma_{(C-H)}$] at 815 cm^{-1} and C=C in-the-plane deformation

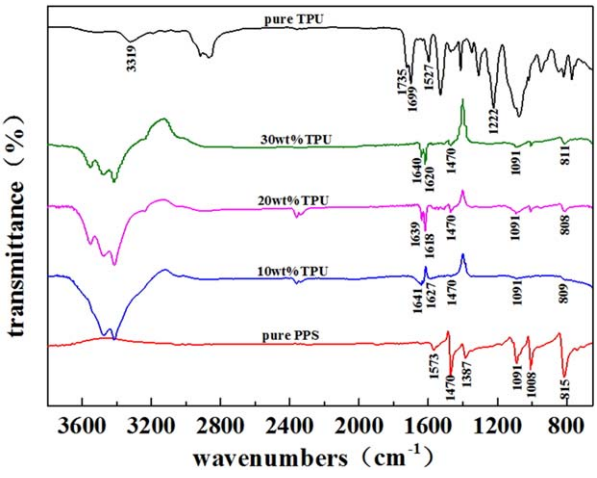

Figure 8. FTIR spectra of TPU, PPS and PPS/TPU composites. [Color figure can be viewed in the online issue, which is available at wileyonlinelibrary.com.]

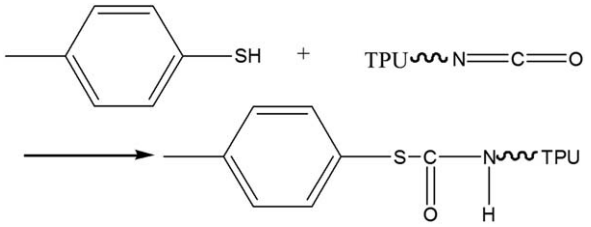

Figure 9. Schematic of the possible reaction between TPU and PPS.

vibration [$\beta_{(C=C)}$] of benzene ring at 1008 cm^{-1}.[22] The characteristic peaks of pure TPU, locating at 3319,1699, 1527 and 1211 cm^{-1} due to $\delta_{(H)}$ and $\nu_{(C=O)}$,[23,24] disappear in the PPS/TPU composites. The three peaks located at 809, 1008 and 1470cm^{-1}, assigned to benzene ring frame stretching vibrations, can be observed in pure TPU and PPS/TPU composites in comparison to the pure PPS. However, $\gamma_{(C-H)}$ happens to offset at about 815–808 cm^{-1}. It is noted that there are two new peaks located at about 1640 cm^{-1} and 1620 cm^{-1} in the PPS/TPU composites compared with the pure TPU and PPS. The peak at about 1620 cm^{-1} is associated with ν(C=O) shift of the peak at 1699 cm^{-1} in the pure TPU due to the mediator effect affected by sulfur atom. The peak at about 1640 cm^{-1} may be associated with urea hydroxyl produced from allophanate (1735 cm^{-1}) in the process which may remain in the pure TPU raw materials. In addition, it is interesting that the intensity of C—S stretching vibration (1091 cm^{-1}) in PPS enhances as increasing concentrations of TPU.

Based on the above experimental results, the possible toughening mechanism for Sr-ferrite/PPS/TPU composites is proposed. Figure 9 shows the mechanism of TPU acting on PPS in the composite system. The TGA and IR analysis of the PPS/TPU composites shows that the urethane connecting hard segments and soft segments disappears producing the isocyanate group (—CNO) from the hard segments of TPU at the temperature of 290 °C during the melt blending. Meantime, S—H bonds exiting at the end region of PPS[25] can react with isocyanate groups[24,26] to produce S—C=O bonds, which is in agreement with the results of the intensity change of C—S stretching vibrations and the shift of $\nu_{(C=O)}$ from 1699 cm^{-1} to about 1620 cm^{-1} in the PPS/TPU composites as shown in Figure 8.

There is no apparent distinction in the SEM micrographs of fractural surfaces in TPU/PPS/Sr-ferrite ternary system due to the small content of PPS matrix in comparison with the filler contents, as shown in Figure 2. However, the fractural surfaces of PPS/TPU system display some different morphologies. Figure 10 shows the SEM micrographs of fractural surfaces of the different PPS/TPU composites prepared by HAAKE torque rheometer. Except the common feature of a large amount of holes generated during the melt-blending process, smooth fractural surface occurs in the pure PPS sample as shown in Figure 10(a), which indicates the evident characteristics of the brittle fractural behavior dominated by microcracks. However, the rugged fractural morphologies are observed in the samples with the addition of TPU as shown in Figure 10(b–d), which implies that the IS of PPS/TPU system has a major improvement. This microstructure difference also explains the improvement of IS in the Sr-ferric/PPS/TPU system as shown in Figure 1.

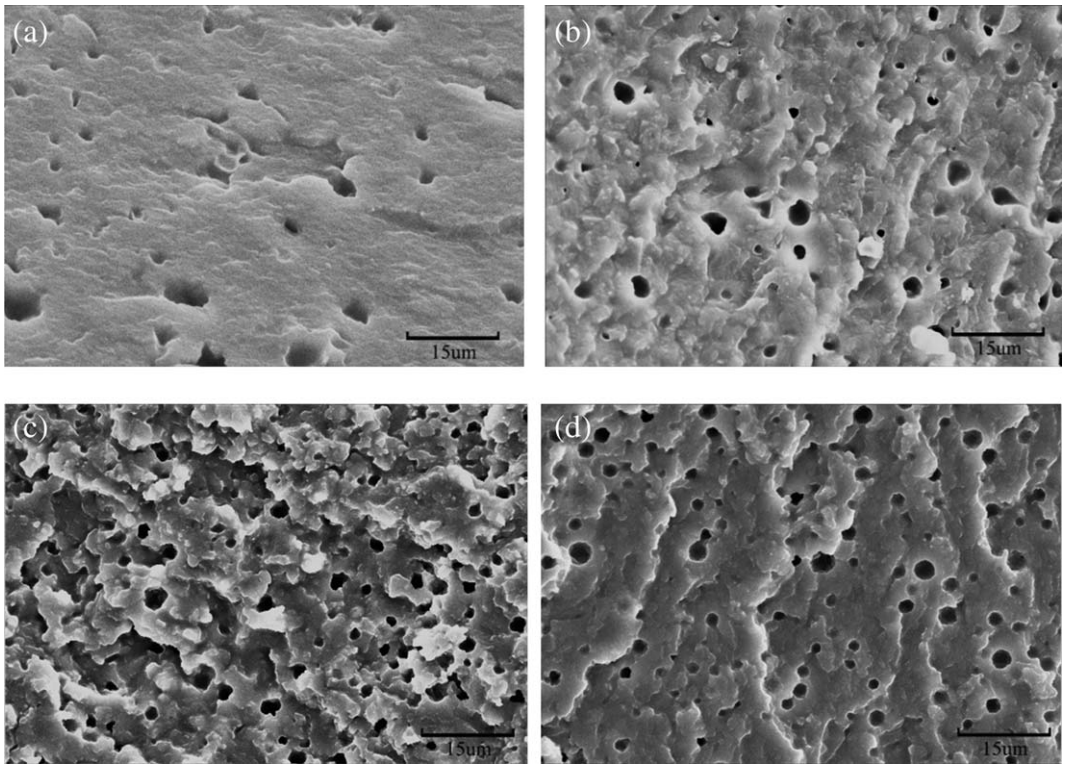

Figure 10. SEM micrographs of fractural surface of PPS/TPU composites of (a) pure PPS, (b) 10 wt % TPU/PPS composite, (c) 20 wt % TPU/PPS composite, and (d) 30 wt % TPU/PPS composite.

Figure 11 shows the BSE micrographs of fracture surface of 30 wt % TPU/PPS. The whole image has the homogeneous contrast, which exhibits that no conspicuous phase separation occurs between PPS and TPU even in the sample with 30 wt % TPU addition. This indirectly proves the good compatibility between TPU and PPS and the different mechanism from the present theory of elastomer toughening the brittle plastics as a separate phase.[27,28]

CONCLUSIONS

TPU effectively improves the IS of Sr-ferrite/PPS/TPU ternary composite though it partly decomposes at the high processing temperature of PPS. By controlling the additions of TPU, composites with improved toughness can be achieved. The IS is achieved to be 5.77 kJ/m^2 increased by around 51.44% when the content of TPU reaches to 11 wt %. The SEM patterns reveal the good compatibility between TPU and PPS. The action mechanism of TPU on PPS is proposed and discussed based on the experimental results. The hard segments of TPU decompose during the melt blending and generate the isocyanate groups (—CNO), which reacts with the end group (S—H) in PPS. Due to the graft of PPS molecular chains by TPU, the IS and thermal stability are improved. This is different from the conventional toughening mechanism by the conformation of elastomers and the suppression of microcracks propagation.

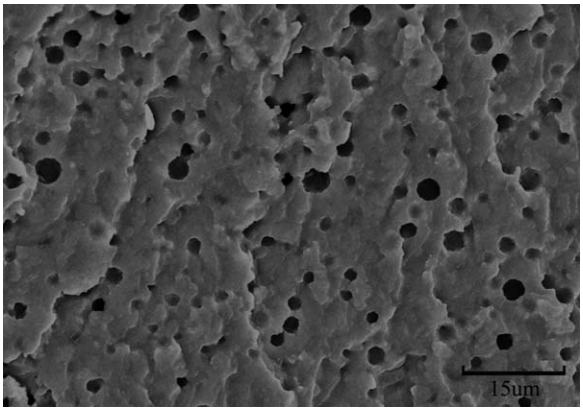

Figure 11. BSE micrograph of fractural surface of 30 wt % TPU/PPS composite.

REFERENCES

1. Hamano, M. *J. Alloys Compounds* **1995**, *222*, 8.
2. Ormerod, J.; Constantinides, S. *J. Appl. Phys.* **1997**, *81*, 4816.
3. Díez-Pascual, A. M.; Naffakh, M.; Marco, C.; Ellis, G. *Compos. Part A: Appl. Sci. Manuf.* **2012**, *43*, 603.
4. Díez-Pascual, A. M.; Naffakh, M. *Mater. Chem. Phys.* **2012**, *135*, 348.
5. Mengden, D. *Quality* **1988**, *27*, 56.
6. Kubo, K.; Masamoto, J. *Kobunshi Ronbunshu* **1999**, *56*, 426.
7. Tong, W.; Yang, J.; Wang, X. J.; Wei, W. U.; Guang-Xian, L. I. *China Plast. Ind.* **2006**, *34*, 51.
8. Zhang, Z. J.; Yang, J.; Chen, Z. J.; Gong, J. B. *China Plast. Ind.* **2014**, *7*, 20.

9. Montes, S.; Carrasco, P. M.; Ruiz, V.; Cabañero, G.; Grande, H. J.; Labidi, J.; Odriozola, I. *Compos. Sci. Technol.* **2015**, *117*, 26.
10. Liang, J.; Li, R. *J. Appl. Polym. Sci.* **2000**, *77*, 409.
11. Koo, K. K.; Inoue, T.; Miyasaka, K. *Polym. Eng. Sci.* **1985**, *25*, 741.
12. Palanivelu, K.; Balakrishnan, S.; Rengasamy, P. *Polym. Test.* **2000**, *19*, 75.
13. Zhang, S. L.; Wang, D.; Guan, S. W.; Jiang, Z. H.; Wu, Z. W.; Wang, G. B. *Mater. Lett.* **2007**, *61*, 267.
14. Ajili, S. H.; Ebrahimi, N. G.; Khorasani, M. T. *J. Appl. Polym. Sci.* **2003**, *89*, 2496.
15. Lu, J.; Huang, R.; Oh, I. K. *Macromol. Chem. Phys.* **2007**, *208*, 405.
16. Tanaka, H.; Kunimura, M. *Polym. Eng. Sci.* **2002**, *42*, 1333.
17. Herrera, M.; Matuschek, G.; Kettrup, A. *Polym. Degrad. Stabil.* **2002**, *78*, 323.
18. Lu, D.; Yang, Y.; Zhuang, G.; Zhang, Y.; Li, B. *Macromol. Chem. Phys.* **2001**, *202*, 734.
19. Bora, M.; Çoban, O.; Avcu, E.; Fidan, S.; Sınmazçelik, T. *Polym. Compos.* **2013**, *34*, 1591.
20. Chen, Z.; Li, T.; Yang, Y.; Liu, X.; Lv, R. *Wear* **2004**, *257*, 696.
21. Zhang, R. C.; Xu, Y.; Lu, A.; Cheng, K.; Huang, Y.; Li, Z. M. *Polymer* **2008**, *49*, 2604.
22. Yu, J.; Asai, S.; Sumita, M. *J. Macromol. Sci., Part B* **2000**, *39*, 279.
23. Cai, L.; Tong, D.; Lin, Z. *Polym. Mater. Sci. Eng.* **2011**, *27*, 79.
24. Pielichowski, K.; Leszczyńska, A. *J. Therm. Anal. Calorim.* **2004**, *78*, 631.
25. Zhao, Q.; Wen, Y.; Wang, Y.; Liu, M.; Luo, N.; Wang, W.; Li, X. *Polym. Mater. Sci. Eng.* **2007**, *23*, 141.
26. Kawaguchi, K.; Tajima, Y. *J. Appl. Polym. Sci.* **2006**, *100*, 4375.
27. Liu, H.; Zhang, J. *J. Polym. Sci. Part B: Polym. Phys.* **2011**, *49*, 1051.
28. Mehrabzadeh, M.; Rezaie, D. *J. Appl. Polym. Sci.* **2002**, *84*, 2573.